Assisted Dual-Power Transmission of Bipolar DC Microgrid Using Idle Open-Winding PMSM Drives

Yuge Song, Jiadong Lu, *Senior Member, IEEE*, Yihua Hu, *Senior Member, IEEE*, Ao Zhang, Sidi Chen, and Mohammed Alkahtani, *Senior Member, IEEE*

***Abstract*—The voltage unbalance and instability of a bipolar dc microgrid affect the service life of electrical equipment. The integration method of power transmission on the load side can both accurately adjust the load voltage and save costs. However, most methods are functionally limited, which makes it difficult to balance and stabilize voltage simultaneously. If the existing integration methods are used to ensure power quality, the coordination among multiple idle motors or the method of adjusting topologies repeatedly is required, which makes the system more complex and less efficient. In this article, a dual-power transmission multiplexing (DPTM) system is proposed, where the dual functions, voltage balance, and energy storage are integrated into the open-winding permanent magnet synchronous motor (OW-PMSM) drive. The DPTM system can simultaneously balance voltage and store energy in case of an idle motor. Besides, auxiliary current reversal and auxiliary task mixed assignment algorithms with the residual winding are proposed, which can adapt to the changes of the system voltage and switch tasks online. Its effectiveness under different operation conditions is confirmed experimentally on a 1 kW OW-PMSM drive.**

***Index Terms*—Bipolar dc microgrid, dual power transmission multiplexing (DPTM) system, energy storage, voltage balance.**

I. Introduction

DC microgrid is superior in reducing energy conversion and improving energy efficiency and system reliability [1]. With more voltage output levels and higher power transmission efficiency, bipolar dc microgrids have attracted a lot of attention in recent years [2], [3]. Distributed new energy generations and loads can also more flexibly select the appropriate voltage level (PO, ON, or PN) to be connected to the bipolar dc microgrid. However, due to the fact that new energy power generations are affected by the environment and have intermittent and fluctuating characteristics, they lead to unstable and unbalanced voltage in the bipolar dc microgrid. Meanwhile, the frequent switching and asymmetric distribution of loads on the power grid also exacerbate the voltage instability and imbalance problems of the bipolar dc microgrid, as shown in Fig. 1. Voltage instability and imbalance problems cause damage and increase losses to the system and electrical equipment [4], [5]. If balance between power generation and power consumption is ensured, these problems of unstable and unbalanced voltage can be alleviated. The existing methods can alleviate the above-mentioned problems from two aspects: adjusting power generation and adjusting load, as shown in Fig. 1.

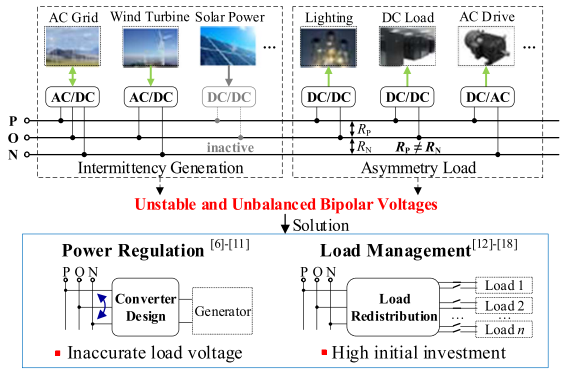

Fig. 1. Bipolar DC microgrid and related research.

The first type is power regulation, which is usually fulfilled by designing a converter [6], [7], [8], [9], [10], [11]. In [6], four voltage balancer topologies have been proposed. In [7] and [8], a full-bridge three-level dc–dc converter is designed to replace a dedicated voltage balance converter. Literature [9] proposes a three-phase active rectifier that can independently stabilize and balance voltage. In [10], a triple-active-bridge converter is proposed with an automatic voltage balancing capability for bipolar dc distribution. In [11], a neutral line drop compensation method is proposed, which compensates for the fluctuation and voltage drop on the dc line by means of the current and impedance of the neutral line. However, the converter is often integrated in the generation device rectifier, which can only adjust the voltage on the power side. Meanwhile, redundant power switches or

Received 18 February 2025; revised 29 May 2025 and 10 July 2025; accepted 12 August 2025. Date of publication 18 August 2025; date of current version 22 October 2025. This work was supported in part by Shaanxi Provincial Natural Science Basic Research Program Project under Grant 2024JC-YBMS-406, in part by the Innovation Foundation for Doctor Dissertation of Northwestern Polytechnical University under Grant CX2024068, and in part by the Outstanding Doctoral Dissertation Cultivation Fund of the School of Automation, Northwestern Polytechnical University. Recommended for publication by Associate Editor K. Chen. *(Corresponding author: Jiadong Lu.)*

Yuge Song, Jiadong Lu, Ao Zhang, and Sidi Chen are with the School of Automation, Northwestern Polytechnical University, Xi'an 710129, China (e-mail: songyuge@mail.nwpu.edu.cn; j.d.lu@nwpu.edu.cn; aozhang@mail.nwpu.edu.cn; chensidi@mail.nwpu.edu.cn).

Yihua Hu is with the Department of Engineering, King's College London, WC2R 2LS London, U.K. (e-mail: yihua.hu@kcl.ac.uk).

Mohammed Alkahtani is with the Department of Electrical Engineering, College of Engineering, University of Bisha, Bisha 61922, Saudi Arabia (e-mail: mskahtani@ub.edu.sa).

Color versions of one or more figures in this article are available at https://doi.org/10.1109/TPEL.2025.3599254.

Digital Object Identifier 10.1109/TPEL.2025.3599254

converters are used to improve the reliability of the system, which increases the cost and complexity of the system.

To adjust the load terminal voltage more accurately, the second is load management. The distributed dc electric springs [12], [13], [14], [15] are introduced at the positive and negative dc load nodes, which can reduce the unbalance of the system by flexibly adjusting the power of noncritical loads. However, these methods are limited to the power of noncritical loads. Considering power limitation, in literatures [16], [17], and [18], the method of load redistribution is adopted. However, the initial investment in such a method has also remarkably increased.

Although a respective optimal solution can be found from the generation side or load side for different bipolar dc microgrid systems, high costs are inevitable. This may be overcome by means of the idea of integration. If a large number of electrical equipment on the load side can be used for power transmission, the load voltages can be stable and balanced, and the risk of dedicated converter failure can be avoided. Besides, most power transmission devices are designed with their own controllers and measurement sensors, so the controllers and sensors can be shared to save costs.

In recent years, the integration of power transmission has been studied, and relevant research works can be divided into two categories, i.e., energy storage unit reuse and motor drive reuse. In [19] and [20], the charging port of an electric vehicle is designed as a bidirectional dc/dc converter, and the energy storage system in an idle electric vehicle is used for dc microgrid. However, this method makes the converter complicated and increases the volume and weight of the original system. Considering that there are a large number of ac drive systems [21] on the load side and they are designed with the same components and working properties as power conversion modules [22], they fully have the potential to integrate power conversion functions. In [23] and [24], the charging device is replaced by integrating the charging function with the drive inverter. In [25], [26], [27], [28], and [29], different kinds of motor drives charge the energy storage devices. Due to the limits on background, in the above study, only the flow of power from the grid to the battery charging process is considered. In [30], inactive motor drive system is reused for voltage balance, and rapid bipolar voltage regulation is realized by changing motor topology and adjusting control methods. The method of rotor position preset is also proposed to avoid the jitter problem caused by the change of current direction during operation. However, the proposed method can achieve only one function, and the position preset method takes a long time, as shown in Fig. 2.

It is feasible and promising to use a multiplex motor drive system to regulate voltage. However, there are few research works on the multiplexing of bidirectional dc/dc converter, and there are some defects in the research of voltage balance multiplexing. Meanwhile, different topologies and conflicting transmission paths make it impossible to realize dual-function transmission directly through a combination. Coordination between multiple idle motors or method of adjusting topologies repeatedly may balance and stabilize voltage simultaneously, but it makes the system more complex and less efficient. A permanent magnet synchronous motor (PMSM) drive system is

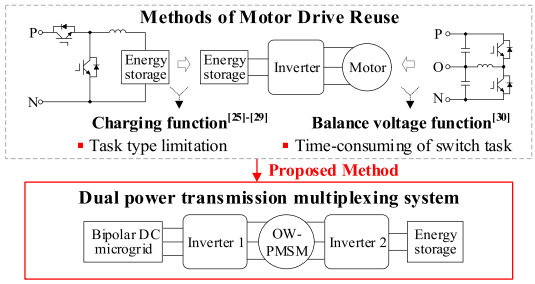

Fig. 2. Integration methods of power transmission.

widely used in electrified transportation, wind power generation, high-precision servo system, and many other fields because of its excellent operation performance, high power density, and high efficiency. However, the power of the motor is still restricted by the power of the inverter. Therefore, a structure of an open-winding permanent magnet synchronous motor (OW-PMSM) is proposed. OW-PMSM inherits the merits of PMSM [31] and open-winding structure [32], which shows a good application prospect. Compared with the traditional PMSM structure, under the fixed bus voltage, the OW-PMSM drive system has a wider speed range, more flexible control, and higher fault tolerance. Meanwhile, OW-PMSM independent phase windings and redundant phase legs of the dual inverter are naturally superior in realizing the power transmission multiplexing function. The OW-PMSM drive system is reused in the charging process [33]. There are a few research works on dual-function power transmission of the OW-PMSM drive system.

In this article, based on the topology of the OW-PMSM drive, a dual-power transmission multiplexing (DPTM) system is proposed, as shown in Fig. 2. Compared with conventional methods, the DPTM system can integrate both a bidirectional dc/dc converter and a voltage balancer simultaneously. According to the variable voltages of the bipolar dc microgrid, the proposed method can flexibly assign and switch tasks. Meanwhile, to solve rotor jitter caused by power transmission task change in mixed tasks, the methods of auxiliary task mixed assignment (ATMA) and auxiliary current reversal (ACR) with the residual winding are proposed. The proposed method can replace a partial bidirectional dc/dc converter and voltage balancer, contribute to voltage stabilization and balance, reduce system complexity, improve system stability and reliability, and improve power component utilization of the OW-PMSM drive system.

This article is organized as follows. In Section II, the topology of the DPTM system is given. The DPTM control method is proposed in Section III. The implementation and discussion are described in Section IV. In Section V, experimental results are presented. Conclusions are given finally in Section VI.

II. Topology of DPTM System

A. Topology

There are three key points to construct the topology: 1) introduce the neutral interface of the bipolar dc microgrid and the interface of the energy storage system; 2) determine the position of current and voltage sensors; and 3) keep the original

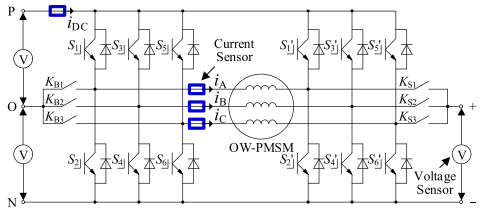

Fig. 3. Topology of the proposed DPTM method.

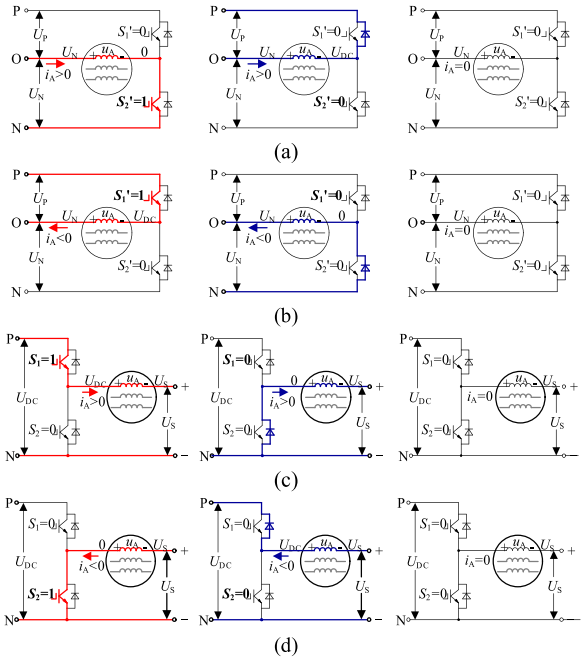

Fig. 4. Four basic working types of phase A. (a) LtoU. (b) UtoL. (c) GtoE. (d) EtoG.

OW-PMSM driving capability. The DPTM topology proposed in this article is shown in Fig. 3, where S_x and S'_x are power switches ($x = \{1, 2, 3, 4, 5, 6\}$), K_{By} and K_{Sy} are relay switches (y = {1, 2, 3}), and P, O, and N are, respectively, connected to the positive, zero, and negative connections of the bipolar dc microgrid. + and − connect the positive and negative terminals of the energy storage system, respectively. The positions of current sensors and voltage sensors are shown in Fig. 3.

B. Four Basic Working Types

When the motor is idle and power transmission needs to be completed, the proposed topology is changed by controlling K_{By} and K_{Sy}. Every winding can realize dual functions of voltage balance and energy storage. Each task can be divided into two types based on the positive or negative direction of the power transmission current, where the positive direction of current is specified in Fig. 3. Therefore, each phase winding has four basic working types, i.e., lower to upper pole (LtoU), upper to lower pole (UtoL), grid to energy storage system (GtoE), and energy storage system to grid (EtoG).

Taking phase A as an example, the implementation stages of the four basic working types are shown in Fig. 4. When K_{B1} is connected and K_{S1} is disconnected, phase A is used for the voltage balancer. The charging state, discharging state, and possible current discontinuity state of LtoU and UtoL are, respectively, shown in Fig. 4(a) and (b). Similarly, When K_{S1} is connected and K_{B1} is disconnected, phase A is used for the bidirectional dc/dc converter. The charging state, discharging state, and possible current discontinuity state of GtoE and EtoG are shown in Fig. 4(c) and (d), respectively. It is worth noting that the neutral point O is disconnected from the DPTM system. Power transmission is related to U_{DC} ($U_{DC} = U_P + U_N$) but not to either U_P or U_N alone. Therefore, the neutral point O is ignored in Fig. 4(c) and (d).

Therefore, when the system performs the positive task (LtoU or GtoE), the three phase voltages u_A, u_B, and u_C are shown in (1). When the system performs the negative task (UtoL or EtoG), u_A, u_B, and u_C are shown in (2)

$$u_A = \begin{cases} K_{B1}\left[U_N - (1 - S'_2)\, U_{DC}\right] + K_{S1}\left(S_1 U_{DC} - U_S\right), i_A > 0 \\ 0, i_A \le 0 \end{cases}$$

$$u_B = \begin{cases} K_{B2}\left[U_N - (1 - S'_4)\, U_{DC}\right] + K_{S2}\left(S_3 U_{DC} - U_S\right), i_B > 0 \\ 0, i_B \le 0 \end{cases}$$

$$u_C = \begin{cases} K_{B3}\left[U_N - (1 - S'_6)\, U_{DC}\right] + K_{S3}\left(S_5 U_{DC} - U_S\right), i_C > 0 \\ 0, i_C \le 0 \end{cases} \tag{1}$$

$$u_A = \begin{cases} K_{B1}\left(U_N - S_1 U_{DC}\right) + K_{S1}\left[(1 - S_2)\, U_{DC} - U_S\right], i_A < 0 \\ 0, i_A \ge 0 \end{cases}$$

$$u_B = \begin{cases} K_{B2}\left(U_N - S_3 U_{DC}\right) + K_{S2}\left[(1 - S_4)\, U_{DC} - U_S\right], i_B < 0 \\ 0, i_B \ge 0 \end{cases}$$

$$u_C = \begin{cases} K_{B2}\left(U_N - S_5 U_{DC}\right) + K_{S3}\left[(1 - S_6)\, U_{DC} - U_S\right], i_C < 0 \\ 0, i_C \ge 0 \end{cases} \tag{2}$$

where K_{By} and K_{Sy} are the switching states of the corresponding relay, respectively, S_x and S'_x are the switching states of power switches, with 1 ON and 0 OFF, U_P, U_N, and U_{DC} are the upper pole, lower pole, and total voltage of the bipolar dc microgrid, and U_S indicates the voltage of energy storage system.

It is worth noting that when this topology is used for power transmission functions, the current is generally continuous, and there is no last dangling state, as shown in Fig. 4.

C. Two Working Modes

According to the three-phase winding task type, the operating mode can be divided into single and mixed operation modes.

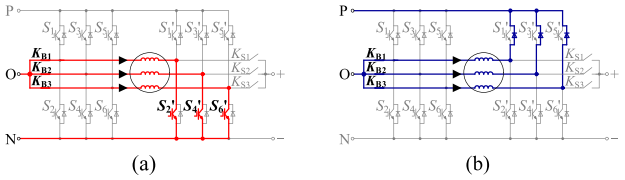

Fig. 5. Balancing voltage process. (a) Charging stage. (b) Discharging stage.

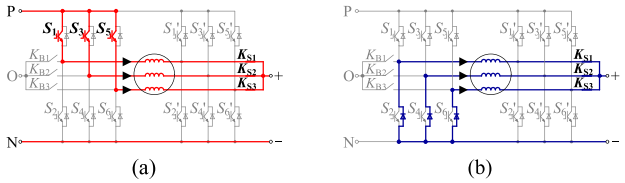

Fig. 6. Stabilized voltage process. (a) Charging stage. (b) Discharging stage.

When the DPTM system is used as a voltage balancer in single operation mode, it is required to connect K_{B1}, K_{B2}, and K_{B3}, and disconnect K_{S1}, K_{S2}, and K_{S3}. Taking LtoU, for instance, Fig. 5 shows the power transmission process. The charging stage is shown in Fig. 5(a), where the power switches S_2', S_4', and S_6' are turned ON, and the lower pole charges the motor windings. The discharging stage is shown in Fig. 5(b), where the power switches S_2', S_4', and S_6' are turned OFF, and the windings discharge to the upper pole through the diodes. Similarly, the task UtoL can be performed by controlling S_1', S_3', and S_5'.

If the DPTM system is only used for energy storage, K_{S1}, K_{S2}, and K_{S3} are connected when K_{B1}, K_{B2}, and K_{B3} are disconnected. Taking GtoE, for instance, the power transmission process is shown in Fig. 6. The charging stage is shown in Fig. 6(a), where the power switches S_1, S_3, and S_5 are turned ON, and the grid charges the motor windings. The discharging stage is shown in Fig. 6(b), where the power switches S_1, S_3, and S_5 are turned OFF to complete the discharge of inductors to the energy storage system through the diodes. Similarly, the task GtoE can be performed by controlling S_2, S_4, and S_6.

The DPTM system is often required to work in mixed operation mode, which can be stable and balanced at the same time. From the above analysis, it can be seen that the switches K_{Sy} and K_{By} on the same phase are repulsive. As a result, the single-phase motor winding can only complete one task at a time. Fortunately, since the power switches controlled by each task are relatively independent, each phase winding can complete its own power transfer task independently. There are 24 different winding assignment tasks for the four mixed tasks, as given in Table I.

For example, phase A alone completed LtoU, and phases B and C jointly completed GtoE. The topology is shown in Fig. 7, in which switches K_{S1}, K_{B2}, and K_{B3} are disconnected, and switches K_{B1}, K_{S2}, and K_{S3} are connected. In Fig. 7(a), S_2', S_3, and S_5 are turned ON, and the bipolar dc microgrid and the lower pole of grid charge the motor windings simultaneously. In Fig. 7(b), S_2', S_3, and S_5 are turned OFF, and the motor windings discharge to the storage energy system and the upper pole through the diodes.

TABLE I
DIFFERENT WINDING ASSIGNMENT TASKS OF MIXED TASKS

	A	B	C	A	B	C	A	B	C
1	LtoU	GtoE	GtoE	GtoE	LtoU	GtoE	GtoE	GtoE	LtoU
	GtoE	LtoU	LtoU	LtoU	GtoE	LtoU	LtoU	LtoU	GtoE
2	LtoU	EtoG	EtoG	EtoG	LtoU	EtoG	EtoG	EtoG	LtoU
	EtoG	LtoU	LtoU	LtoU	EtoG	LtoU	UtoL	UtoL	GtoE
3	UtoL	GtoE	GtoE	GtoE	UtoL	GtoE	GtoE	GtoE	UtoL
	GtoE	UtoL	UtoL	UtoL	GtoE	GtoE	UtoL	UtoL	GtoE
4	UtoL	EtoG	EtoG	EtoG	UtoL	EtoG	EtoG	EtoG	UtoL
	EtoG	UtoL	UtoL	UtoL	EtoG	UtoL	UtoL	UtoL	EtoG

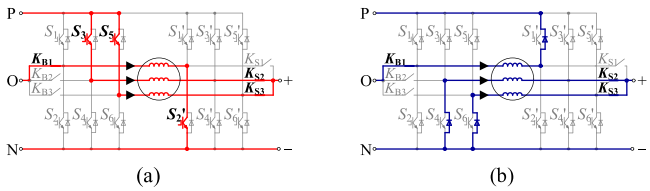

Fig. 7. Power transfer process in mixed operation mode. (a) Charging stage. (b) Discharging stage.

To sum up, in single operation mode, the number of working phases in the DPTM system needs to be determined, and in mixed operation mode, the task distribution mode is diverse and complicated. Besides, grid voltage fluctuations cause changes in task size or type switching during motor windings. As the amplitude or direction of the inductor current changes, unnecessary jitter may arise in the motor rotor. Thus, the DPTM control algorithm needs to be discussed.

III. DPTM CONTROL ALGORITHM

A. Analysis of Stability Points

The conventional PMSM drive system can directly determine the rotor position according to the combined direction of the three-phase currents. However, the open-winding structure leads to zero sequence current in DPTM system, which generates zero sequence torque. As a result, it is necessary to analyze the effect of zero sequence current on the system. Torque is the force that supports motor rotation when the motor is driven. In the power transmission task, the role of torque is to position the motor rotor in a fixed position according to the relationship between the three-phase currents. Therefore, it is crucial to find these fixed locations for different currents.

For nonpolar motors, the equation of torque is as follows:

$$T_e = \frac{3}{2} n_p \left[i_q \psi_{f1} - 6 i_0 \psi_{f3} \sin(3\theta) \right] \tag{3}$$

where n_p is the number of pole-pairs, ψ_{f1} and ψ_{f3} are the fundamental and third harmonic component amplitudes of the rotor flux linkage, respectively, i_q stands for the q-axis current, i_0 stands for the zero sequence current, and θ denotes the electrical angle of the motor rotor.

The constant amplitude variation matrix from the three-phase stationary ABC coordinate frame to the synchronous rotating dq0 coordinate frame is mentioned in [31]; thus, the relationship

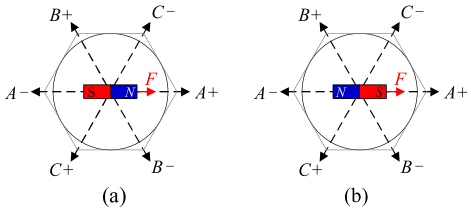

Fig. 8. Rotor force with $T_e = 0$. (a) Steady stage. (b) Unsteady stage.

between i_d, i_q, i_0 and i_A, i_B, i_C is

$$\begin{bmatrix} i_d \\ i_q \\ i_0 \end{bmatrix} = \frac{2}{3} \begin{bmatrix} i_A\cos(\theta) & i_B\cos(\theta - 2\pi/3) & i_C\cos(\theta + 2\pi/3) \\ -i_A\sin(\theta) & -i_B\sin(\theta - 2\pi/3) & -i_C\sin(\theta + 2\pi/3) \\ 0.5i_A & 0.5i_B & 0.5i_C \end{bmatrix}. \tag{4}$$

After the coordinate frame is changed, the expression of torque is obtained and simplified as follows:

$$\begin{cases} T_e = & T_q + T_0 \\ T_q = & n_p\left(\left(-i_A + \frac{1}{2}i_B + \frac{1}{2}i_C\right)\sin\theta + \left(\frac{\sqrt{3}}{2}i_B - \frac{\sqrt{3}}{2}i_C\right)\right. \\ & \left.\cos\theta\right)\psi_{f1} \\ T_0 = & -3n_p\left(i_A + i_B + i_C\right)\psi_{f3}\sin(3\theta) \end{cases} \tag{5}$$

where T_q is the torque arising from i_q, and T_0 is the torque arising from i_0.

The expression of T_q is the same as the torque formula of PMSM, so the rotor position can be determined by the combined direction of three phase currents. However, the extra torque T_0 is related to sin(3θ), which undoubtedly increases the complexity of the analysis. Therefore, additional analysis of the effect of T_0 on rotor position is required. According to (5), when θ is 0°, 60°, 120°, 180°, 240°, and 300°, $T_0 = 0$.

However, a position with torque equal to 0 is not necessarily stable. In Fig. 8, the force on both motor rotors is in A+, and the torque is 0. With a slight disturbance, Fig. 8(a) can return to its original position, while Fig. 8(b) cannot.

The torque is specified to add $\Delta\theta$ disturbance. If the motor can still return to the original position, the point is stable; otherwise, it is unstable. Rotor jitter arising from unstable points has a great impact on power transfer [30]. Therefore, the motor jitter shall be avoided.

Taking the rotor position at 0° as an example, when the rotor is subjected to disturbances $\Delta\theta$, the disturbance ΔT_0 is shown in the following equation:

$$\Delta T_0 = -3n_p\left(i_A + i_B + i_C\right)\psi_{f3}\sin(3\Delta\theta). \tag{6}$$

In (6), if $i_A + i_B + i_C > 0$, while the rotor is subjected to positive or negative disturbance of $\Delta\theta$, the torque is negative or positive and the rotor returns to the initial position, thus 0° is the stable point. If $i_A + i_B + i_C < 0$, while the rotor is subjected to positive or negative disturbance of $\Delta\theta$, the torque is positive or negative and the rotor cannot return to the initial position, thus

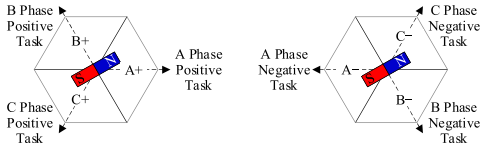

Fig. 9. Initial task assignment method in single operation mode.

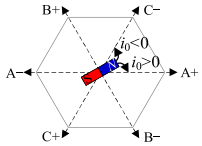

Fig. 10. Effect of T_0 on T_q.

0° is the unstable point. When $i_A + i_B + i_C = 0$, there is no i_0 and T_0. Similarly, it can be discovered from analysis that when $i_A + i_B + i_C > 0$, 0°, 120°, and 240° are stable points, and when $i_A + i_B + i_C < 0$, 60°, 180°, and 300° are stable points. If a negative zero sequence current is injected when the rotor position is 0°, then the 0° position will change from a stable point to an unstable point. The randomness of the disturbance results in that the motor position is not directly determined by the current direction. The rotor may produce position jitter at the time of disturbance. Therefore, the control algorithm needs to be designed to avoid the rotor position uncertainty problem.

B. Initial Task Assignment

In single-task mode, if each of the three phases completes one-third of the target current at the initial stage, the initial position of the motor rotor may be an unstable point. Fortunately, if only one phase winding is used for power transmission tasks, T_q can be used to make the rotor position controllable. In the initial task, the working phase needs to be determined according to the polarity of the target current i_{Target} and the rotor position of the motor, where the current positive direction is shown in Fig. 3. The initial task assignment method in single operation mode is shown in Fig. 9. Taking the rotor position in Fig. 9, when $i_{Target} > 0$, phase A works first; otherwise, phase C works first.

In mixed tasks mode, the rotor position is determined by T_q and T_0 together. At this time, the stability point of the motor cannot be determined solely by i_q. Fortunately, when the i_q direction changes, θ turns 180° electrical angle. While the zero sequence current changes in the opposite direction, θ only rotates 60°. Therefore, T_0 only slightly affects the effect of T_q, without causing rotor jitter in the system. The effect of T_0 on T_q is shown in Fig. 10. When θ is determined by i_q, the rotor deflects in the direction of A+ when $i_0 > 0$. When $i_0 < 0$, the rotor deflects in the C-direction. The maximum deflection electrical angle is 60°. For a motor with $n_p = 4$, the maximum deflection mechanical angle is only 15°. Therefore, in the mixed tasks mode, the effect of zero sequence current on the rotor position can be ignored.

There are multiple distribution methods given in Table I. Therefore, it is necessary to design the initial task assignment. To avoid rotor jitter, the task of each phase needs to be determined

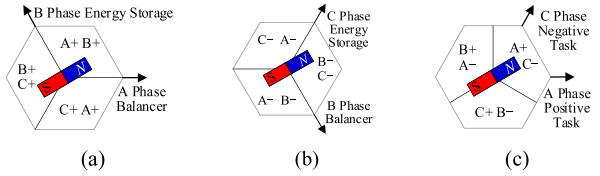

Fig. 11. Initial task assignment method. (a) Same positive polarity. (b) Same negative polarity. (c) Different polarity.

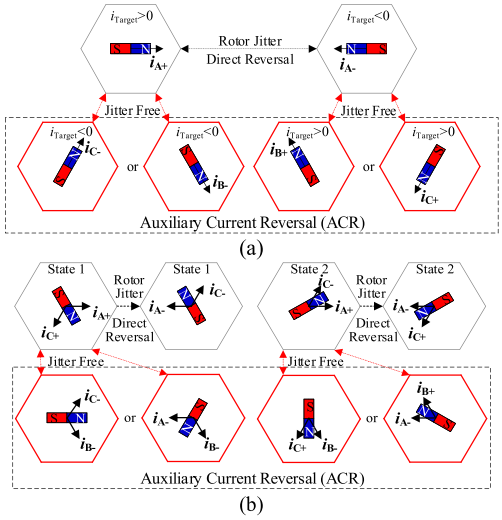

Fig. 12. ACR. (a) In single-task mode. (b) In mixed tasks mode.

according to the polarity of the two tasks and rotor position. Two windings are selected to undertake different tasks in the initial stage. In Fig. 11(a), when the rotor is in three regions [A+, B+), [B+, C+), [C+, A+), the voltage balancer is allocated to phases A, B, and C, respectively, and the energy storage is allocated to phases B, C, and A, respectively. Similarly, in Fig. 11(b), when the rotor is in three regions [B-, C-), [C-, A-), [A-, B-), the voltage balancer is allocated to phase B, C, and A, respectively, and the energy storage is allocated to phase C, A, and B, respectively. The initial task assignment diagram with the opposite polarity of the task is shown in Fig. 11(c). For example, when the electrical angle of the rotor is 30°, the distribution of different tasks is shown in Fig. 11.

C. Auxiliary Current Reversal Method

According to the analysis in Section III-A, if the polarity of the task changes during operation, the unstable operation state may also occur. The single and mixed modes need to be analyzed separately.

In single-task mode, if the task polarity changes, the motor still appears in an unstable state. As shown in Fig. 12(a), when phase A performs the positive task of power transmission, the current of phase A is i_{A+}. At this time, if the load or power supply change of the grid causes the phase A current to reverse directly to i_{A-}, the rotor position will change from stable to unstable. Therefore, the ACR is performed. It is assisted by phase B or C and performs a negative task with i_{B-} or i_{C-}. Similarly, if phase A performs the negative task, the current of phase A is i_{A-}. At this

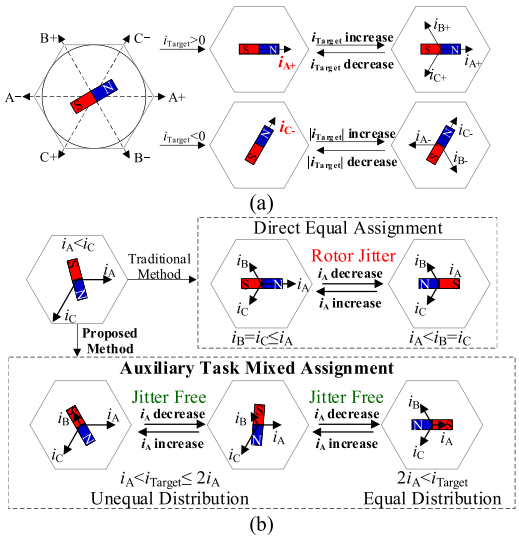

Fig. 13. Auxiliary shunt method. (a) In single-task mode. (b) In mixed tasks mode.

time, if i_{Target} is reversed, it can still be assisted by the phases B and C to perform the positive task, and the current is i_{B+} or i_{C+}.

In mixed tasks mode, the rotor jitter may occur only if the currents of both tasks are reversed simultaneously. In Fig. 12(b), rotor jitter can be generated by direct reversal of the same polarity tasks (State 1) and opposite polarity tasks (State 2). The uncertain state and jitter of the rotor in mixed mode can also be avoided by using the ACR method mentioned above. The residual phase is used to replace one of the phases. Taking phases A and C to complete different tasks as an example in Fig. 12(b), when the i_{Target} direction of the two phases changes at the same time, the task of replacing phase A or C with phase B is used to avoid the rotor jitter.

To sum up, there are many options for auxiliary method. In single-task mode, it is necessary to determine which residual phase assists the current reversal. In mixed tasks mode, it is necessary to determine which working phase is being replaced. The method of initial task assignment mentioned in Section III-B can uniquely determine the assignment method of auxiliary tasks.

The above-mentioned research is aimed at the rotor jitter problem during task switching. However, only two-phase windings are used together at most, and the power transmission capacity of the system is limited. It is necessary to improve the proposed method by using the auxiliary shunt method to improve the power transmission capacity.

D. Auxiliary Shunt Method

To guarantee the high efficiency of the DPTM system, the residual phase needs to assist the power transmission task when the remaining winding does not perform the ACR.

In single-task mode, if θ is determined by i_{q}, the three windings share the current directly, and the rotor stability point remains unchanged, as shown in Fig. 13(a). Therefore, a shunt threshold i_{Thr} is set to ensure that the rotor rotates when the

feedback current of the working phase is greater than i_{Thr}. The shunt threshold i_{Thr} is determined according to different motor systems. Therefore, the minimum value of i_{Thr} should be the minimum current that causes the motor to rotate, which is affected by many factors, such as the friction coefficient, moment of inertia, load, and so on. The minimum of i_{Thr} can also be estimated experimentally. The maximum of i_{Thr} cannot exceed the rated current of the motor in theory. In addition, it is also possible to determine whether the auxiliary phase can be used to assist power transmission by the consistency of the rotor position and the current determination position.

In mixed tasks mode, if only a certain threshold is set for directly bisecting the task, the rotor may jitter. Taking phases A and C to complete different tasks as an example, i_{C} is larger than i_{A}, and then phase B is auxiliary to C. The results of the direct average distribution method are shown in Fig. 13(b). At this time, i_{A} is still larger than the sum of current vectors of the two phases, so the rotor position is at 0°. However, as i_{A} decreases, the vector sum of i_{B} and i_{C} becomes greater than i_{A}. Meanwhile, the rotor position becomes an unstable point. Therefore, the method of ATMA is proposed, where, in addition to the shunt threshold, the current sharing conditions must be set. The principle of setting the shunt threshold is the same as that in single-task mode. There are two current sharing conditions. On the one hand, i_{Target} of the shunt phase needs to break through the limit of the current sharing threshold, where the current balancing threshold must be set so that the rotor position can be controlled before the flow balancing. On the other hand, i_{Target} of the shunt phase is greater than two times of the other. If i_{Target} of one task is greater than the other and reaches the shunt threshold, then the remaining phase assists 30% (unequal distribution) of this task. As i_{Target} increase, the remaining phase contributes to 50% (equal distribution) of the task after the current sharing condition is met. The effect of the ATMA method is shown in Fig. 13(b). The larger i_{C} is shared as i_{Target}. If the i_{Target} is less than $2i_{\mathrm{A}}$, the remaining phase only gets 30% of the task. If the i_{Target} is greater than $2i_{\mathrm{A}}$, the remaining phase is divided into 50% of the task.

IV. Implementation and Discussion

A. Application Scenario

The motor drive systems may be idle for a long time, such as the electric vehicle drive system, flywheel energy storage systems, a redundantly designed motor drive system, and a motor drive system with a specific function. The motor drive systems in all these application scenarios have the potential to serve as reusable power transmission functions. Motor drive systems that have been idle for a long time are given priority to be reused for power transmission functions. Different motor drive systems can set thresholds according to the rated load, which can ensure the controllability of the motor rotor even under unpredictable loads. The quantitative metrics, such as rotor position deviation, response time, and jitter amplitude, are mostly determined by the PI parameters and inertia during the dynamic adjustment process. The system can adjust the PI parameters according to its own different requirements. If the system needs to strictly avoid rotor jitter, multiple DPTM systems can be combined for use, performing only a single task or a task with a fixed current direction.

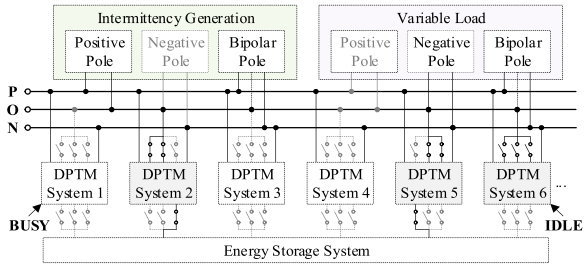

Fig. 14. Overall control strategy diagram.

For higher power levels, all the OW-PMSM drive systems on the power grid can be regarded as a large system. The proposed topology only requires the addition of six relays to transform the traditional OW-PMSM drive system into a DPTM system. The DPTM system is divided into two types: "BUSY" and "IDLE." Among them, "BUSY" is used for the normal driving mode, while "IDLE" can be reused for power transmission tasks, as shown in Fig. 14. The idle DPTM systems select the task form according to the specific situation of the bipolar dc microgrid. In Fig. 14, the idle DPTM systems 2 and 5 perform mixed tasks, while the idle DPTM system 6 only performs the voltage balancing task. When any of the DPTM systems needs to perform driving work, disconnect the corresponding relay to execute the control command. The proposed DPTM system is no different from the traditional OW-PMSM driver system. When the control task is completed, the relay can be reconnected to assist in the power transmission task of the power grid.

The research of this article mainly focuses on the study of the power transmission control method of the single DPTM system. In a multi-DPTM system, if individual motors are still controlled separately, it will cause fluctuations in grid voltage and power transmission current, affecting the system performance. Therefore, in multi-DPTM cooperative control, control methods such as centralized or decentralized can be selected. It is worth noting that this article only analyzes the power transmission method of a single motor and does not involve the control method of multi-DPTM system.

B. Implementation

The DPTM system topology and the detailed process of the DPTM control algorithm are described in Sections II and III. Depending on the control objective, choose whether to operate in single-task mode or mixed mode. Different modes of operation can be divided into initial task assignment, ACR control method, auxiliary shunt method, and end stage. To clearly illustrate the proposed method, the flowchart of the proposed DPTM method is shown in Fig. 15, where $i_{\mathrm{Target\_B}}$ and $i_{\mathrm{Target\_S}}$ represent the target voltage balance current and the target storage current, respectively. i_{Thr} is the shunt threshold. If the proposed system performs the single operation mode, select "or" in the flowchart "or/and" and choose the corresponding target current $i_{\mathrm{Target\_B}}$

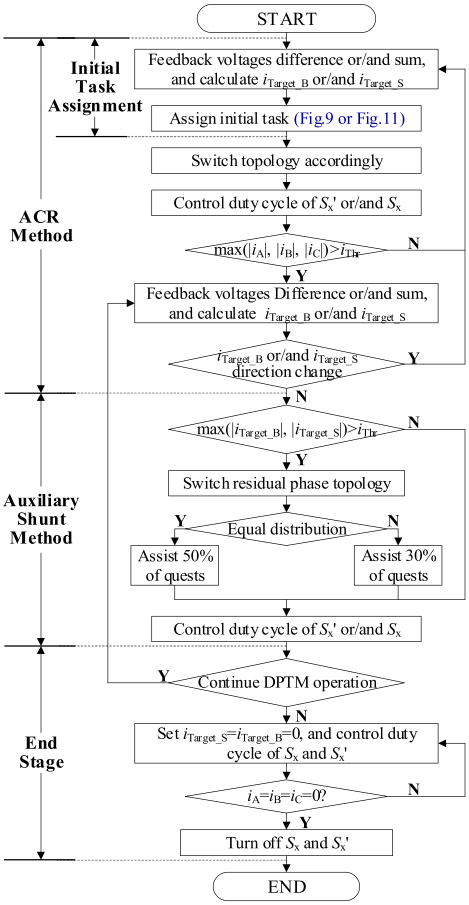

Fig. 15. Flowchart of the proposed DPTM method.

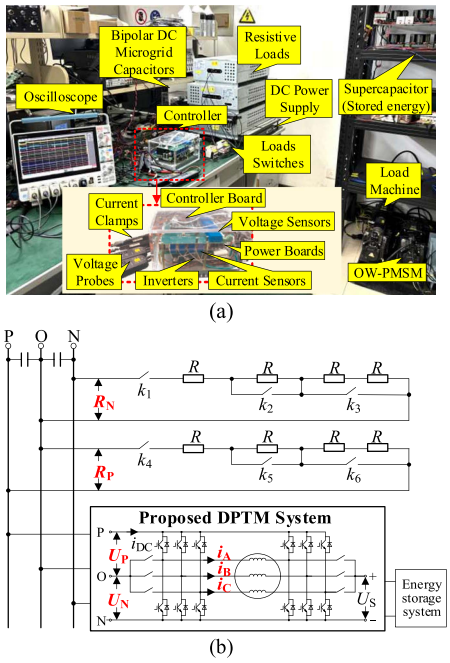

Fig. 16. Experimental setup. (a) Platform. (b) Platform architecture.

or $i_{\mathrm{Target\_S}}$. If the mixed operation mode is performed, select "and" in the flowchart "or/and."

C. Discussion

First, the impact of parameter variations, especially motor winding resistance and inductance, on the performance of the DPTM system is analyzed. The change of resistance value will cause a loss change during the system power transmission. The inductance change is mainly reflected at the microlevel, such as current ripple. The system adopts voltage and current double closed-loop control, so the parameter change in the control process only affects the intermediate variable but does not affect the final control effect. Therefore, the effect of the mutual inductance change of the motor on the system can also be negligible.

Besides, the cost of the system is discussed. The voltage change of the grid system is usually relatively slow, so the topology change is not required to be fast. Topological changes can be achieved with relays, avoiding the use of additional power electronics. The system adds six relays to the traditional OW-PMSM system, which can directly realize dual-function transmission without increasing the volume and cost of the system. The low-cost topological transformation also increases the utilization rate of the original power components.

Finally, the efficiency of the system needs to be discussed. A remarkable feature of PMSM is high efficiency. In the stable state, the motor basically does not rotate, so the iron consumption can be ignored. According to the voltage of the grid, only part of the power of the motor is used, so the copper consumption is lower than the rated loss. In addition, the skin effect of direct current used for power transmission is less obvious. Therefore, the efficiency is high for the motor system. Besides, the effect of different working modes is only related to the size and direction of the current. To further reduce the loss, the current of the power transmission can also be reduced. The shunt threshold and current sharing threshold set in this article also reduce the switching loss of the system to a certain extent and improve the efficiency.

V. Experimental Results

To validate the correctness and effectiveness of the proposed DPTM topology and method, an experimental platform is set up, as shown in Fig. 16(a). The upper and lower poles of a bipolar dc microgrid are formed by four capacitors in parallel. A dc power supply (TDK G300-11.5-1P208-M) provides a 200 V voltage (U_{set}) for the bipolar dc microgrid P and N poles. The proposed DPTM system is mainly composed of the OW-PMSM drive system and six additional relays. The OW-PMSM drive system mainly uses its motor windings, two inverters, and a controller to achieve the power transmission process. The parameters of the motor are given in Table II. It is worth noting that when the selected traditional OW-PMSM drive system is transformed into the DPTM system, it is necessary to ensure that the inverter power supply of the motor drive system matches the P and N pole voltages of the bipolar dc microgrid. Theoretically, the parameters of the motor do not affect the power transmission function,

TABLE II
MAIN PARAMETERS OF OW-PMSM FOR EXPERIMENT

Parameters	Value	Parameters	Value
Rated Power	1.0 kW	Line Resistance	2.76 Ω
Rated Voltage	220 V	Line Inductance	6.42 mH
Rated Current	4 A	Rated Speed	2500 r/min
Rated Torque	4 N·m	Pole Pairs	4

but they do affect the power transmission performance. In the selection of OW-PMSM, motor windings with large inductance and small resistance should be chosen as much as possible to reduce the current ripple during the power transmission process and improve the power transmission efficiency. Power boards of both controllers and inverters are powered by the P and N poles of bipolar dc microgrids. The power boards supply different voltages required by the control board. The control board integrates the OW-PMSM position signal acquisition, four current sampling signals (LA 25-P), three voltage sampling signals (LV 25-P), six switch control signals, and six pairs of driving signals. The controller adopts DSP TMS320F28377D with a carrier frequency of 20 kHz. The control function is executed every two carrier cycles at a frequency of 10 kHz. Six PWM drive signals are sent to two inverters (PM75RLA120). Relays are used for the task selection of motor windings. When the relay is connected and disconnected, the circuit is in a state of zero voltage and zero current. Therefore, the parameter selection of relays mainly considers the rated current and action-release time. The relays used in this article are JQC-3FF-S-Z. The maximum switching current is 15 A, which is definitely capable of handling the power transmission current. The action and release times are both less than 10 ms. Sufficient switching time should be reserved during task switching. As an energy storage system, the supercapacitors stabilize the voltage of the bipolar dc microgrid. The voltage of the energy storage system must not exceed the total voltage of the bipolar dc microgrid. The experimental platform architecture is shown in Fig. 16(b), where the switches k_1–k_6 simulate the voltage imbalance or insufficiency of bipolar dc microgrid, i_A, i_B, and i_C represent the three-phase current of the motor, i_{DC} represents the dc current of the motor, U_P and U_N represent the upper and lower pole voltage of the bipolar dc microgrid, and U_S represents the voltage of the energy storage. i_{DC} and U_S are used to protect the OW-PMSM drive system and energy storage system, respectively. Bipolar resistors R_P and R_N are modulated to simulate the load imbalance in the grid. The magnitude of the grid voltage, current, or total load $R_P + R_N$ is adjusted to simulate an excess or shortfall of grid energy. It is worth noting that the step size of the adjustment switch is set short to shorten the experiment time. But in theory, the load and power of the grid should not change so frequently.

Since the proposed topology can operate in a single mode or a mixed mode, the experimental part is divided into two parts for verification. On the one hand, the verification of power transmission capability under a single operating mode is divided into two parts: voltage balance and energy storage, as shown in Fig. 17(i). Fig. 18 simulates the situation of grid imbalance by adjusting the size of bipolar loads, verifying the

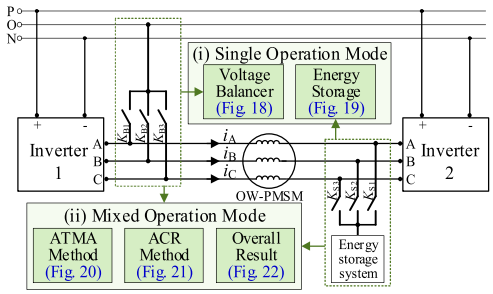

Fig. 17. Experimental verification process.

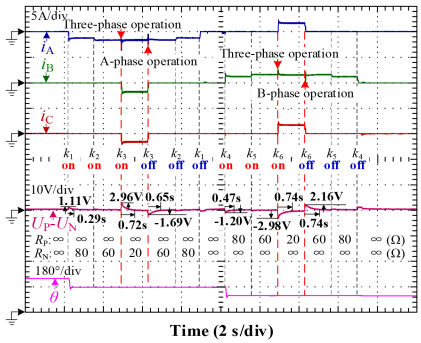

Fig. 18. Voltage balance function of the DPTM system.

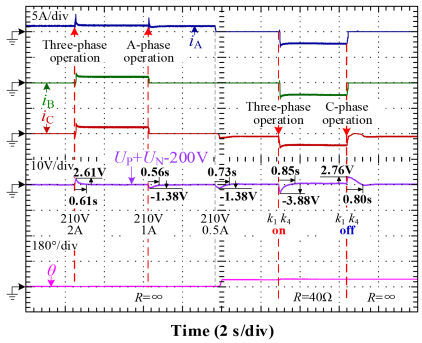

Fig. 19. Energy storage function of the DPTM system.

effectiveness of the DPTM system being used only for voltage balancers. Meanwhile, Fig. 19 simulates the situation of insufficient or excessive power in the power grid by adjusting the imbalance between power generation and consumption in the power grid, verifying the feasibility of the DPTM system being only used for the bidirectional dc/dc converter for energy storage. On the other hand, the verification of the multiplexing effect in the hybrid operation mode is divided into three parts: two algorithms to avoid rotor jitter and the overall result, as shown in Fig. 17(ii). Figs. 20 and 21, respectively, verify the effectiveness of the ATMA and ACR algorithms under mixed operation mode. Fig. 22 simulates the unstable and unbalanced voltage conditions by adjusting the power generation and the size of the bipolar loads, verifying the overall control method of the mixed operation mode. The current clamps (Tektronix TCP0030A), voltage probes (Tektronix TMDP0200), and oscilloscope (Tektronix MOS46) are used for signal sampling and

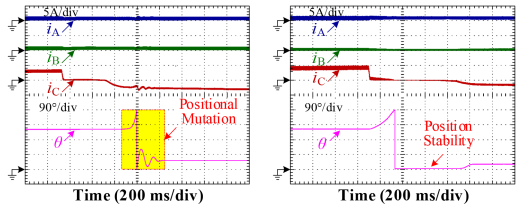

Fig. 20. Different auxiliary power transmission methods. (a) Direct equal distribution method. (b) ATMA method.

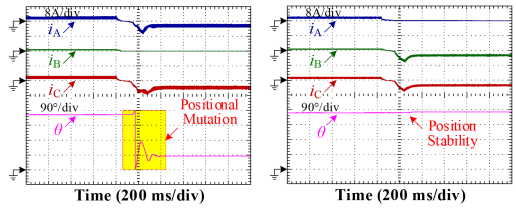

Fig. 21. Effect of target currents reversal on rotor position. (a) Without ACR method. (b) With ACR method.

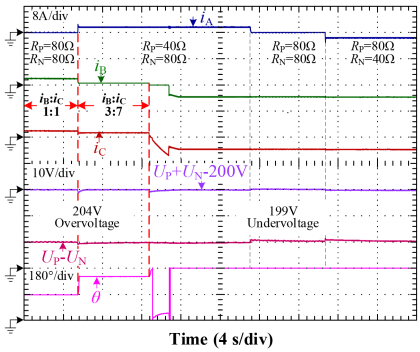

Fig. 22. Mixed operation of the DPTM system.

recording. The proposed method is implemented based on the traditional OW-PMSM drive system. Therefore, corresponding voltage and current protection must exist. In terms of relay control, dead zones for the control signals of two relays on the same winding are also added through software and hardware to prevent both relays from conducting simultaneously. The experimental results only verify the feasibility of a single DPTM system and do not involve the cooperative power transmission method of a multi-DPTM system. The experimental scenarios and detailed experimental processes are described as follows.

First, when the generation and consumption of a bipolar dc microgrid are balanced but the bipolar voltages are unbalanced, or when the OW-PMSM drive system is assigned a single voltage balancing task, K_{B1}, K_{B2}, and K_{B3} need to be connected, and the motor drive system is reused for a single voltage balancing task. To show the effect of the flow sharing threshold, the shunt threshold is set to 2 A. Switch the load switches shown in Fig. 16 to adjust the load imbalance of the bipolar dc microgrid. k_1 is switched ON first, the lower pole is connected to the resistor, and the power grid is unbalanced. Phase A is first used to balance the voltage determined by the rotor position. Then close k_2 and k_3 successively to increase the imbalance of the grid. When k_3 is closed, i_{Target} exceeds the shunt threshold, and the balance control strategy changes from only phase A to three-phase current balancing. Subsequently, disconnect k_3, k_2, and k_1, in turn, with no load at both poles, among which, after k_3 is disconnected, i_{Target} is less than 2 A, and the system returns to only phase A voltage balance function. Similarly, close k_4, k_5, and k_6 successively to increase the imbalance of the grid. Then, disconnect k_6, k_5, and k_4, in turn, with no load at both poles. The experimental results are shown in Fig. 18. According to the imbalance degree of the bipolar dc microgrid, the system can select one phase or three phases for power transmission within a very short time based on the magnitude of the power transmission current. The proposed DPTM system can rapidly balance the bipolar voltage within less than 1 s. The balancing process keeps the voltage difference between the upper and lower poles within a fluctuation range of less than $\pm$ 3 V, not exceeding 3% of the rated voltage of the upper or lower pole (100 V). It is worth noting that the over/undershoot and recovery time are related to the PI parameter. The proposed DPTM system is implemented based on the OW-PMSM drive system, so the current regulation speed is not recommended to be too drastic. Compared with dedicated power transmission devices, its over/undershoot will be larger and the recovery time will be longer. It can be known from Section IV-A that multiple DPTM systems can collaboratively perform the power transmission task. Therefore, both over/undershoot and recovery time will be improved.

Then, when the bipolar voltages in a bipolar dc microgrid are balanced, but the imbalance between power generation and consumption leads to an excess or shortage of power, or when the OW-PMSM drive system is arranged to perform only a single energy storage task, K_{S1}, K_{S2}, and K_{S3} need to be closed, and the motor drive system is used in three bidirectional dc/dc converters. Similarly, the shunt threshold is set to 2 A. The voltage instability of a bipolar dc microgrid is simulated by adjusting the supply current and load R ($R = R_P + R_N$). At the beginning, the power grid is 210 V, 1 A, without load, simulating the situation of excess power grid. i_{Target} does not exceed the shunt threshold, only phase A is used for the dc/dc function to store excess grid energy into the energy storage system. Then, the output current of the power supply is increased to 2 A, and i_{Target} reaches the shunt threshold. Therefore, the system changes from only phase A multiplexing to three-phase simultaneous multiplexing. Then, reduce the power supply current to 1 A, and i_{Target} cannot reach the shunt threshold. The system changed from three-phase multiplexing to only A-phase multiplexing. Continue to reduce the supply current to 0.5 A and switch ON k_1 and k_4 to simulate the power shortage of the grid. Phase C, or three phases, is used to transfer energy from the energy storage system to the grid according to the i_{Target}. Finally, k_1 and k_4 are disconnected and restored to the C-phase power transmission state. The experimental results in Fig. 19 show that the proposed DPTM topology and algorithm can stabilize the voltage of the bipolar dc microgrid quickly. In Fig. 19, when the power supply capacity is sufficient or insufficient, or when the load changes slightly or drastically, the system can select the power

transmission mode within a short period of time according to the magnitude of the power transmission current. Similarly, the proposed topology can rapidly stabilize the grid voltage within less than 1 s. While ensuring rapid voltage stabilization, it can also control the fluctuation within ±4 V and not exceeding 2% of the rated voltage (200 V).

It has been proven that the proposed method can be fast and stable in a single task. However, in more cases, imbalance and instability coexist in the bipolar dc microgrid. At this point, the proposed DPTM system needs to be used in a mixed operation mode. In addition, in situations where the voltage is slightly unbalanced or unstable, and where a single idle motor can balance and stabilize the voltage, a mixed operation mode will also be selected to simplify the control process. As analyzed in Section III-D, compared with the single operation mode, the conventional direct equal assignment method of the mixed operation mode leads to more severe rotor jitter, which endangers the motor drive system. Therefore, the effects of the ATMA control algorithm and the ACR control algorithm before and after their use are compared, respectively, and the effectiveness of the mixed operation mode after adding these two algorithms is verified.

To verify the effectiveness of the proposed ATMA method, the change in electrical angle of the rotor in the conventional method and the proposed method is compared, where the A winding performs the voltage balancing task and the C winding performs the energy storage task. The load switches k_4 and k_6 are turned ON (upper pole with 40 Ω load), and the B winding is used as the residual phase to help the phase A perform power transmission tasks. Then the polarity of the C-phase task is reversed. The electrical angles θ under different control methods are shown in Fig. 20. It can be seen from the figure that the ATMA method can solve rotor jitter. It is worth noting that $\theta = 180°$ or 0° are the same point, so the jump in Fig. 20(b) is actually continuous.

In addition, when the target currents of both tasks change simultaneously, the motor rotor jitters. The voltage is set to 204 V, the upper load is 40 Ω, and the lower load is 80 Ω. The lower pole transmits power to the upper pole, and the phase B assists the phase A for voltage balance. Then, turn the direction of the voltage imbalance, that is, the upper pole is connected to the load of 80 Ω, and the lower pole is connected to the load of 40 Ω, and set the voltage to 199 V simultaneously. The direction of voltage balance and energy storage change simultaneously. If phase B is not assisted in ACR, there is rotor jitter, as shown in Fig. 21(a). According to the method presented in this article, phase B should assist phase A to complete the ACR. The results are shown in Fig. 21(b), and the jitter can be eliminated.

The effectiveness of the proposed method is verified under mixed operation mode. Set the power supply to 204 V, 3.5 A. k_1 and k_4 are both ON, and the upper and lower poles are load-balanced, each carrying 80 Ω. Set the shunt threshold to 0.7 A and the current sharing threshold to 2 A. In the initial phase, phase C is used for dc/dc functions. Phase B assisted phase C power transmission. Since the current sharing threshold is exceeded, i_{B} and i_{C} share $i_{\mathrm{Target\_S}}$ equally. Subsequently, k_6 is switched ON, and the bipolar microgrid is unbalanced. Phase A is used for the voltage balancing function. The load on the grid increases, which consumes part of the electricity. The energy stored by the energy storage system becomes smaller, resulting in $i_{\mathrm{Target\_S}}$ less than the sharing current threshold; therefore, i_{B} and i_{C} divide the target current by 3:7. Then, the power supply voltage is reduced to 199 V, and the power grid is insufficient. The phase C current reverses and becomes the energy storage system to deliver energy to the power supply. Because the phase C electrical energy is still greater than the phase A electrical energy, phase B still assists phase C to complete the voltage stabilization work. Since $i_{\mathrm{Target\_S}}$ is greater than 2 A, phases B and C share the task equally. The experimental results in Fig. 22 show that the proposed DPTM system can effectively balance and stabilize the voltage of the bipolar dc microgrid.

TABLE III
COMPARISON RESULTS UNDER SAME TASKS

Parameters	In [34]	In [35]	Proposed Method
Computational requirements	Low	Low	Low
No. of power switches	4	4	0
No. of inductors	1	2	0
No. of capacitors	3	3	1
No. of current sensors	2	2	0
No. of voltage sensors	3	3	2
No. of controllers	1	1	0
Over/Undershoot	Small	Small	Slightly larger
Recovery time	Short	Short	Slightly longer
Transmission capacity	Limited	Fixed	Flexible

Compared with the dedicated dual-function integration method, the proposed DPTM system has some improvements or drawbacks, as given in Table III. Although the proposed method adds ACR and ATMA algorithms to prevent the inevitable jitter of the motor rotor, these auxiliary algorithms are only simple numerical comparisons and do not impose significant computational requirements. The proposed method and the comparison methods are all controlled through dual closed-loop control of voltage and current, so there is no significant difference in the amount of calculation. The proposed method is based on the OW-PMSM drive system, so there is no need to add additional power switches, inductors, current sensors, and controllers. The motor drive system itself comes with capacitors, and the newly added capacitors are those on the energy storage system side. It is worth noting that the newly added voltage sensor is for achieving voltage control. If the DPTM system directly receives current instructions, there is no need to add the voltage sensors. Since the power transmission current of the proposed method flows through the stator of the motor, the rotation of the motor rotor must be taken into account. Therefore, compared with the dedicated methods, the over/undershoot of the proposed method is slightly larger and the recovery time is slightly longer. Besides, since the proposed method can flexibly increase the idle motor drive system to perform reuse tasks, its transmission capacity is more flexible compared to dedicated equipment.

VI. CONCLUSION

To balance and stabilize the load-side voltage accurately and save the cost of detection and control devices, a DPTM system is proposed in this article. The proposed system is based on the OW-PMSM drive and constructs a new topology without

affecting the normal drive of the motor. Besides, ACR and ATMA algorithms are proposed to solve the rotor jitter problem during task transformation. The merits are as follows:

Flexibility: The proposed method can accomplish the tasks of voltage balance and stability independently or simultaneously, so the burden of power transmission can be flexibly shared according to system requirements.

Accuracy: The OW-PMSM drive system, as a common and promising electrical equipment on the load side, can precisely adjust the voltage on the load side.

Cost saving: In the proposed method, the idle OW-PMSM drive of bipolar dc microgrids is fully used without additional power switches.

High efficiency: In the control algorithm, the task assignment ratio and type can be adjusted depending on the change of system voltage.

REFERENCES

[1] T. Dragičević, X. Lu, J. C. Vasquez, and J. M. Guerrero, "DC microgrids—Part II: A review of power architectures, applications, and standardization issues," *IEEE Trans. Power Electron.*, vol. 31, no. 5, pp. 3528–3549, May 2016.

[2] I. N. Jiya, H. Van Khang, N. Kishor, and R. M. Ciric, "Novel family of high-gain nonisolated multiport converters with bipolar symmetric outputs for DC microgrids," *IEEE Trans. Power Electron.*, vol. 37, no. 10, pp. 12151–12166, Oct. 2022.

[3] V. Chapparya, A. Dey, and S. P. Singh, "A novel non-isolated boost-zeta interleaved DC-DC converter for low voltage bipolar DC micro-grid application," *IEEE Trans. Ind. Appl.*, vol. 59, no. 5, pp. 6182–6192, Sep./Oct. 2023.

[4] Y. Lin, F. Zhou, G. Xu, W. Xiong, and G. Ning, "Bipolar current-fed DC–DC converter with automatic voltage balance and full range ZVS for bipolar DC system," *IEEE Trans. Power Electron.*, vol. 39, no. 4, pp. 4248–4259, Apr. 2024.

[5] Q. Tian, G. Zhou, H. Li, Y. Yang, and D. Zhou, "Symmetrical bipolar output isolated four-port converters based on center-tapped winding for bipolar DC bus applications," *IEEE Trans. Power Electron.*, vol. 37, no. 2, pp. 2338–2351, Feb. 2022.

[6] F. Wang, Z. Lei, X. Xu, and X. Shu, "Topology deduction and analysis of voltage balancers for DC microgrid," *IEEE J. Emerg. Sel. Topics Power Electron.*, vol. 5, no. 2, pp. 672–680, Jun. 2017.

[7] G. V. Broeck, J. Beerten, M. D. Vecchia, S. Ravyts, and J. Driesen, "Operation of the full-bridge three-level DC–DC converter in unbalanced bipolar DC microgrids," *IET Power Electron.*, vol. 12, no. 9, pp. 2256–2265, Aug. 2019.

[8] G. V. d. Broeck, W. Martinez, M. Dalla Vecchia, S. Ravyts, and J. Driesen, "Conversion efficiency of the buck three-level DC–DC converter in unbalanced bipolar DC microgrids," *IEEE Trans. Power Electron.*, vol. 35, no. 9, pp. 9306–9319, Sep. 2020.

[9] Y. Li, A. Junyent-Ferré, and J.-M. Rodriguez-Bernuz, "A three-phase active rectifier topology for bipolar DC distribution," *IEEE Trans. Power Electron.*, vol. 33, no. 2, pp. 1063–1074, Feb. 2018.

[10] N. Naseem and H. Cha, "Triple-active-bridge converter with automatic voltage balancing for bipolar DC distribution," *IEEE Trans. Power Electron.*, vol. 37, no. 7, pp. 8640–8648, Jul. 2022.

[11] T.-H. Jung, G.-H. Gwon, C.-H. Kim, J. Han, Y.-S. Oh, and C.-H. Noh, "Voltage regulation method for voltage drop compensation and unbalance reduction in bipolar low-voltage DC distribution system," *IEEE Trans. Power Del.*, vol. 33, no. 1, pp. 141–149, Feb. 2018.

[12] Y. Yang, S.-C. Tan, and S. Y. R. Hui, "Mitigating distribution power loss of DC microgrids with DC electric springs," *IEEE Trans. Smart Grid*, vol. 9, no. 6, pp. 5897–5906, Nov. 2018.

[13] K.-T. Mok, M.-H. Wang, S.-C. Tan, and S. Y. R. Hui, "DC electric springs—A technology for stabilizing DC power distribution systems," *IEEE Trans. Power Electron.*, vol. 32, no. 2, pp. 1088–1105, Feb. 2017.

[14] J. Liao, N. Zhou, Y. Huang, and Q. Wang, "Unbalanced voltage suppression in a bipolar DC distribution network based on DC electric springs," *IEEE Trans. Smart Grid*, vol. 11, no. 2, pp. 1667–1678, Mar. 2020.

[15] J. Liao, N. Zhou, Y. Huang, and Q. Wang, "Decoupling control for DC electric spring-based unbalanced voltage suppression in a bipolar DC distribution system," *IEEE Trans. Ind. Electron.*, vol. 68, no. 4, pp. 3239–3250, Apr. 2021.

[16] J.-O. Lee, Y.-S. Kim, and S.-I. Moon, "Current injection power flow analysis and optimal generation dispatch for bipolar DC microgrids," *IEEE Trans. Smart Grid*, vol. 12, no. 3, pp. 1918–1928, May 2021.

[17] B. S. H. Chew, Y. Xu, and Q. Wu, "Voltage balancing for bipolar DC distribution grids: A power flow based binary integer multi-objective optimization approach," *IEEE Trans. Power Syst.*, vol. 34, no. 1, pp. 28–39, Jan. 2019.

[18] J. Liao, N. Zhou, Q. Wang, and Y. Chi, "Load-switching strategy for voltage balancing of bipolar DC distribution networks based on optimal automatic commutation algorithm," *IEEE Trans. Smart Grid*, vol. 12, no. 4, pp. 2966–2979, Jul. 2021.

[19] K.-W. Hu and C.-M. Liaw, "Incorporated operation control of DC microgrid and electric vehicle," *IEEE Trans. Ind. Electron.*, vol. 63, no. 1, pp. 202–215, Jan. 2016.

[20] Y. Xuan, X. Yang, W. Chen, T. Liu, and X. Hao, "A novel three-level CLLC resonant DC–DC converter for bidirectional EV charger in DC microgrids," *IEEE Trans. Ind. Electron.*, vol. 68, no. 3, pp. 2334–2344, Mar. 2021.

[21] X. Li, S. Zhang, C. Zhang, Y. Zhou, X. Yuan, and Y. Dong, "Model predictive control with duty ratio modulation for open-winding PMSM drives with common DC bus," *IEEE Trans. Power Electron.*, vol. 38, no. 12, pp. 15287–15299, Dec. 2023.

[22] V. F. Pires, A. Cordeiro, C. Roncero-Clemente, S. Rivera, and T. Dragičević, "DC-DC converters for bipolar microgrid voltage balancing: A comprehensive review of architectures and topologies," *IEEE J. Emerg. Sel. Topics Power Electron.*, vol. 11, no. 1, pp. 981–998, Feb. 2023.

[23] M. Eull, L. Zhou, M. Jahnes, and M. Preindl, "Bidirectional nonisolated fast charger integrated in the electric vehicle traction drivetrain," *IEEE Trans. Transp. Electrific.*, vol. 8, no. 1, pp. 180–195, Mar. 2022.

[24] T. Payarou and P. Pillay, "Integrated multipurpose power electronics interface for electric vehicles," *IEEE Trans. Transp. Electrific.*, vol. 9, no. 2, pp. 2429–2443, Jun. 2023.

[25] Z. Yu, C. Gan, K. Ni, Y. Chen, and R. Qu, "Dual-electric-port bidirectional flux-modulated switched reluctance machine drive with multiple charging functions for electric vehicle applications," *IEEE Trans. Power Electron.*, vol. 36, no. 5, pp. 5818–5831, May 2021.

[26] M. Tong, M. Cheng, S. Wang, and W. Hua, "An on-board two-stage integrated fast battery charger for EVs based on a five-phase hybrid-excitation flux-switching machine," *IEEE Trans. Ind. Electron.*, vol. 68, no. 2, pp. 1780–1790, Feb. 2021.

[27] H. J. Raherimihaja, Q. Zhang, G. Xu, and X. Zhang, "Integration of battery charging process for EVs into segmented three-phase motor drive with V2G-mode capability," *IEEE Trans. Ind. Electron.*, vol. 68, no. 4, pp. 2834–2844, Apr. 2021.

[28] C. Li, W. Huang, R. Cao, F. Bu, and C. Fan, "An integrated topology of charger and drive for electric buses," *IEEE Trans. Veh. Technol.*, vol. 65, no. 6, pp. 4471–4479, Jun. 2016.

[29] F. Yu, Q. Yin, Z. Zhu, and X. Cheng, "A multienergy interface electric-drive-reconstructed onboard charger for EVs with integrated control strategy," *IEEE Trans. Power Electron.*, vol. 39, no. 4, pp. 4050–4061, Apr. 2024.

[30] J. Lu, Y. Hu, Y. Song, Y. Su, J. Wang, and J. Liu, "Assisted power transfer for voltage balance of bipolar DC microgrids using inactive motor drives," *IEEE Trans. Ind. Electron.*, vol. 69, no. 12, pp. 12129–12139, Dec. 2022.

[31] Y. Zhou and H. Nian, "Zero-sequence current suppression strategy of open-winding PMSG system with common DC bus based on zero vector redistribution," *IEEE Trans. Ind. Electron.*, vol. 62, no. 6, pp. 3399–3408, Jun. 2015.

[32] C. Zhang et al., "Zero-sequence current suppression method for fault-tolerant OW-PMSM drive with asymmetric zero-sequence voltage injection," *IEEE Trans. Ind. Electron.*, vol. 70, no. 3, pp. 2351–2362, Mar. 2023.

[33] S. Foti, A. Testa, G. Scelba, S. De Caro, and L. D. Tornello, "A V2G integrated battery charger based on an open end winding multilevel configuration," *IEEE Open J. Ind. Appl.*, vol. 1, pp. 216–226, 2020.

[34] L. Tan, B. Wu, V. Yaramasu, S. Rivera, and X. Guo, "Effective voltage balance control for bipolar-DC-bus-fed EV charging station with three-level DC–DC fast charger," *IEEE Trans. Ind. Electron.*, vol. 63, no. 7, pp. 4031–4041, Jul. 2016.

[35] S. Kim, H. Cha, and H.-G. Kim, "High-efficiency voltage balancer having DC–DC converter function for EV charging station," *IEEE J. Emerg. Sel. Topics Power Electron.*, vol. 9, no. 1, pp. 812–821, Feb. 2021.

Yuge Song was born in Shaanxi, China, in 1998. She received the B.S. degree in electrical engineering from Northwest Agriculture and Forestry University, Yangling, China, in 2020. She is currently working toward the Ph.D. degree in electrical engineering with Northwestern Polytechnical University, Xi'an, China.

Her research interests include motor drivers, power electronics, and calibration of sensors in permanent magnet synchronous motor drives.

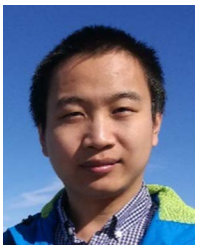

Jiadong Lu (Senior Member, IEEE) was born in Pucheng, China, in 1990. He received the B.S., M.S., and Ph.D. degrees in electrical engineering from Northwestern Polytechnical University (NWPU), Xi'an, China, in 2012, 2015, and 2018, respectively.

Between 2017 and 2018, he was with the Department of Electrical Engineering, Electronics and Computer Science, University of Liverpool, Liverpool, U.K., as an Honorary Academic Researcher. He is currently an Associate Research Fellow with the Department of Electrical Engineering, NWPU. His research interests include hybrid-fault-tolerant control techniques for permanent magnet synchronous motor drives, aging issues for motor drives, and power electronics converters and control.

Yihua Hu (Senior Member, IEEE) received the B.S. degree in electrical engineering and the Ph.D. degree in power electronics and drives, both from the China University of Mining and Technology, Jiangsu, China, in 2003 and 2011, respectively.

Between 2011 and 2013, he was with the College of Electrical Engineering, Zhejiang University, as a Postdoctoral Fellow. Between 2013 and 2015, he was a Research Associate with the Power Electronics and Motor Drive Group, University of Strathclyde. Between 2016 and 2019, he was a Lecturer with the Department of Electrical Engineering and Electronics, University of Liverpool (UoL). Between 2019 and 2023, he was a Reader and Electrical Engineering Group Head with the Electronics Engineering Department, The University of York (UoY). He is currently a Reader with King's College London (KCL). He has authored or coauthored more than 160 papers in the IEEE transactions journals. His research interests include renewable generation, power electronics converters and control, electric vehicle, more electric ship/aircraft, smart energy system, and nondestructive test technology.

Dr. Hu is an Associate Editor for IEEE TRANSACTIONS ON INDUSTRIAL ELECTRONICS, *IET Renewable Power Generation*, *IET Intelligent Transport Systems,* and *Power Electronics and Drives*. He is a Fellow of the Institution of Engineering and Technology and a Member of the U.K. Young Academy. He was awarded the Royal Society Industry Fellowship.

Ao Zhang was born in Shanxi, China, in 2001. He received the B.S. degree in electrical engineering in 2023 from Northwestern Polytechnical University, Xian, China, where he is currently working toward the master's degree in electrical engineering.

His research interests include permanent magnet synchronous motor drive and power electronics converters and control.

Sidi Chen was born in Jiangsu, China, in 2001. She received the B.S. degree in electrical engineering from Northeast Forestry University, Harbin, China, in 2023. She is currently working toward the M.S. degree in electrical engineering with Northwestern Polytechnical University, Xi'an, China.

Her research interests include motor drivers, power electronics, and integrated battery chargers.

Mohammed Alkahtani (Senior Member, IEEE) received the B.Eng., M.Sc., and Ph.D. degrees in electrical and electronics engineering from Liverpool John Moores University, Liverpool, U.K., and the University of Liverpool, Liverpool, U.K., in 2014, 2016, and 2021, respectively.

In 2014, he became a Member of the Saudi Council of Engineers (SCE). He has more than five years of working experience in the industry worldwide, with many applications of innovative products. He is an Assistant Professor with the Department of Electrical Engineering, College of Engineering, University of Bisha, Bisha, Saudi Arabia. His research interests include the management of photovoltaic and PV array efficiency improvement, artificial intelligence, and algorithms for energy management systems.